High power plasma interaction with tungsten grades in ITER relevant conditions

2015 J. Phys.: Conf. Ser. 591 012030

(http://iopscience.iop.org/1742-6596/591/1/012030)

Journal of Physics: Conference Series **591** (2015) 012030 doi:10.1088/1742-6596/591/1/012030

High power plasma interaction with tungsten grades in ITER relevant conditions

I E Garkusha[1], V A Makhlaj[1], N N Aksenov[1], O V Byrka[1], S V Malykhin[2], A T Pugachov[2], B Bazylev[3], I Landman[3], G Pinsuk[4], J Linke[4], M Wirtz[4], M J Sadowski[5] and E Skladnik-Sadowska[5]

[1] Institute of Plasma Physics, NSC Kharkov Institute of Physics and Technology, Kharkov, Ukraine;
[2] National Technical University "Kharkov Polytechnical Institute", Kharkov, Ukraine;
[3] Karlsruhe Institute of Technology, IHM, P.O. Box 3640, 76021 Karlsruhe, Germany;
[4] Forschungszentrum Juelich GmbH, EURATOM Association, 52425 Juelich, Germany;
[5] National Centre for Nuclear Research (NCBJ), 05-400 Otwock, Poland

E-mail: garkusha@ipp.kharkov.ua

Abstract. Experimental simulations of ITER-like transient events with relevant surface heat load parameters (energy density up to 1.1 MJ/m^2 and the pulse duration of 0.25 ms) as well as particle loads (varied in wide range from 10^{23} to 10^{27} ion/m^2 s) were carried out with a quasi-stationary plasma accelerator QSPA Kh-50. Particular attention was paid to elaboration of damage of tungsten as a main candidate material for ITER divertor surfaces and also as prospective material for DEMO design. Erosion features, cracks evolution and changes in their thickness with increasing exposition dose are studied for different W grades, including deformed material with elongated grains, as well as WTa5 and sintered tungsten.

1. Introduction

Tungsten is considered now as plasma facing material (PFM) for ITER divertor and also it is primary choice for DEMO design [1]. Key advantages of W material are low sputtering yield and tritium retention, high sputtering threshold energy and melting temperature, good thermal conductivity etc. However its brittleness, high ductile to brittle transition temperature (DBTT), ability to melt during the transient events and large Z are among critical issues for tungsten application in fusion reactor [2,3]. Under the high heat loads macroscopic mechanisms of W erosion would be dominating rather than microscopic ones. Macroscopic erosion due to the brittle destruction (cracks, debris and dust particles), tungsten melt losses caused by melt motion and droplets splashing, material modification and changed properties after the repetitive plasma pulses, possible synergetic effects from heat and particle loads require comprehensive studies in ITER relevant conditions [4,5].

Database of tungsten behavior under the high heat loads from the existing machines is insufficient. Only few tokamaks have experience with W. The expected ITER loads (especially for disruption) will considerably exceed the available energy loads in the experimental devices. Resulting damage effects from million ELMs in ITER also remain to be among key topics of predictive studies. Thus fundamental understanding of plasma-surface interaction (PSI) processes in magnetic confinement

devices requires dedicated R&D activity in plasma simulators used in close connection with material characterization facilities as well as with theory and modeling activities [5-7]. For such investigations different simulators of transient loads are now involved (quasi-stationary plasma accelerators, e-beams, dense plasma foci and plasma guns), that are cost effective, flexible, able to provide faster results and important comparison of damage features from various machines [8-13].

While a number of unresolved issues in plasma edge physics (e.g. scrape-off layer, plasma flows and turbulent transport) can only be addressed in tokamaks, issues related to fuel retention, dust formation, impact of transient heat loads on materials, erosion and re-deposition mechanisms, as well as new material concepts can be explored using dedicated PSI devices. Besides a good access to the plasma-material interaction zone, allowing specific diagnostics to be operated and an easy exchange of material samples, the reasons to explore PSI issues using this approach include the ability of plasma simulators to achieve ITER relevant particle and energy fluxes, provide well diagnosed test cases for plasma wall interaction codes benchmarking, as well as test beds for PSI diagnostics.

Thus, using the pool of existing plasma accelerators, guns, e-beam facilities allows contribute to the knowledge-based understanding of the performance and adequacy of candidate plasma facing materials of next step fusion devices under extreme energy and particle load conditions. Such activity is in progress now within IAEA CRP "Investigations of Materials under High Repetition and Intense Fusion-Relevant Pulses" which includes, in particular, round-robin tests of candidate materials in available simulators as well as investigation of combined plasma treatments of samples in different devices.

This paper presents the results of tungsten samples exposures in ITER relevant conditions that have been performed with powerful plasma streams generated by quasi-stationary plasma accelerator QSPA Kh-50. The targets were exposed to a varied number of pulses (up to 400) of different energy load Q. Also we compare the behavior of samples of different grades of tungsten subjected to plasma loads, including those with deformed elongated grains that is chosen as ITER reference material.

2. Experimental setup

Experimental simulations of ITER ELMs with relevant surface heat load parameters (energy density and the pulse duration) as well as particle loads were carried out with a quasi-stationary plasma accelerator QSPA Kh-50 described elsewhere [14-16]. Hydrogen plasma streams, generated by QSPA Kh-50, are injected into the magnetic system of 1.6m in length and 0.44m in inner diameter with a magnetic field of up to 0.54T in diagnostic chamber (2.3m from accelerator) where the target has been installed [14-16]. General view of the experimental installation and scheme of the targets exposure are presented in Fig.1. Plasma parameters were varied both by changing dynamics and the amount of gas filled in the accelerator channel and by the variation of the working voltage of capacitor battery of the discharge in accelerating channel.

Main plasma diagnostics used in the present experiments were as follows: The plasma stream velocity was measured by the time-of-flight of the plasma stream between two magnetic probes and/or photodiodes, the electron density in the plasma stream was evaluated on the basis of Stark broadening of the H_β and H_α spectral lines, radial distributions of the plasma stream energy density were monitored with a movable thermocouple calorimeters. Plasma pressure was measured with piezoelectric detectors. The power density was calculated on the basis of measurements of the time dependencies of the plasma pressure, plasma stream density and its velocity.

For ELM simulations, the main parameters of the plasma stream were as follows: ion impact energy 0.4-0.6 keV, plasma stream density mean plasma density (5-7)x10^{15} cm^{-3}, maximum plasma pressure ~0.32 MPa and the plasma stream diameter 0.18 m. It allows achievement of very small pressure gradient values in the target region, where plasma pressure is practically constant. The plasma pulse shape is triangular with pulse duration of 0.25 ms. Experiments were performed with several fixed surface energy loads chosen in the range of 0.45-1.1 MJ/m^2 (measured precisely with

calorimetry) i.e. either below the melting threshold, or resulted in strong melting of exposed surface [16].

Deformed W grade (Plansee AG), including both single (F) and double forged (DF) samples, was used for the plasma loads tests. Cylindrical shaped specimens with a diameter of 12 mm and a height of 5 mm were prepared from a 1 m long rod (Ø 12 mm, the deformation axis along the rod) [17]. The grain orientation was parallel to the heat transfer direction, which corresponds to the ITER specification. Sintered tungsten samples and WTa5 tungsten that consist of pure tungsten alloyed with 5 wt% tantalum were investigated also.

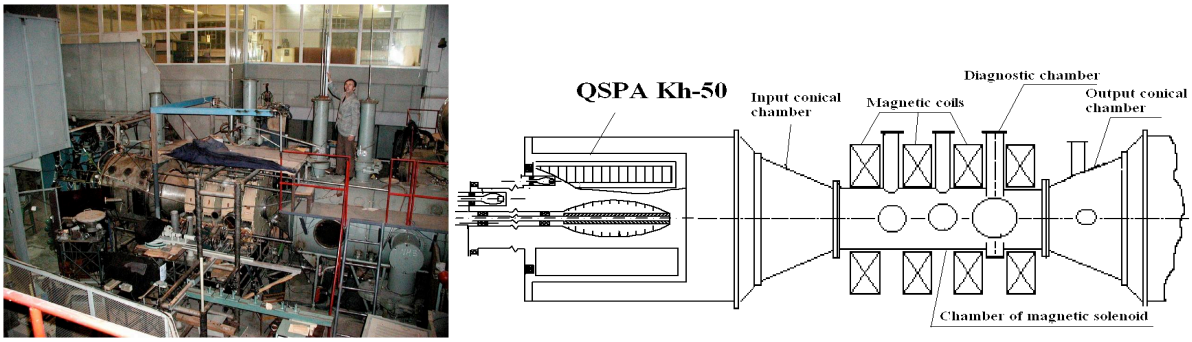

Figure 1. General view of QSPA Kh-50 and scheme of the samples exposures

Before each plasma pulse the sample was kept either under the room temperature (RT) or preheated at T_0 = 200 ^{0}C. The Ohmic heater was installed at the back side of the target. It provided the target heating in vacuum conditions (to avoid oxidation) prior to the exposure. A molybdenum diaphragm with the hole diameter of 1 cm was applied to protect the target edges from plasma impact providing a reference line for profilometry measurements and also to simulate the case when the target size exceeds the diameter of the plasma stream.

Observations of plasma interactions with exposed surfaces have been performed with a high-speed 10 bit CMOS pco.1200 s digital camera PCO AG (exposure time from 1μs to 1s, spectral range from 290 to 1100 nm). Information from consecutive camera frames with traces of particles flying from the tungsten surface after plasma shot allowed calculation of velocities of emitted particles and the time moments of their start-up from the target surface.

Surface analysis was carried out with an optical microscopy, SEM, AFM and profilometry. Measurements of weight losses and microhardness of the surface were performed also. XRD method was applied for structure analysis and measurements of stresses in thin surface layer (X-ray tensometry).

3. Results of experiments

For studies of tungsten response to the plasma exposures, which are not resulted in surface melting, the energy load Q=0.45 MJ/m^2 has been applied. All tungsten grades that have initially room temperature suffer from the major crack meshes which are developed on the surface. Cracking leads to increasing surface roughness as it is measured with profilometry. Evolution of surface roughness for DF samples in the course of plasma exposures is shown in Fig.2. Fluctuation peaks on profilograms correspond to the average distance between developed major cracks. With increasing number of exposures depth and width of the profile fluctuations grow.

Plasma exposures of tungsten in conditions of pronounced melting of the surface layer have been performed with energy load of 0.75 MJ/m^2. Corresponding changes in the profile of the surface after 10 plasma pulses are presented in Fig.3. Smoothing crack edges due to the melting is observed by profilometry. However surface roughness after plasma exposures with surface melting is essentially higher in comparison with similar number of pulses with heat load below the melting threshold.

Besides major cracks, micro-cracks network along the grain boundaries is always detected in experiments. It is attributed to the surface melting and following resolidification. Typical cell sizes of intergranular micro-cracks network are within 10–40 μm, which corresponds to the grain size of the W grade.

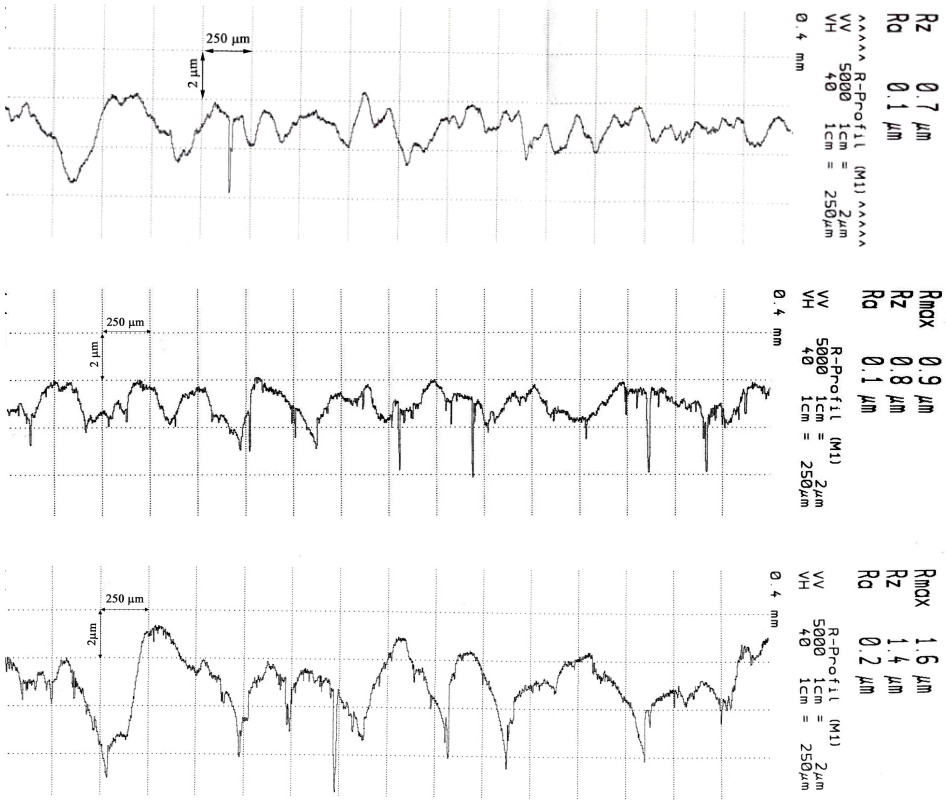

Figure 2. Surface profile development in the course of plasma exposures, Q=0.45 MJ/m^2.

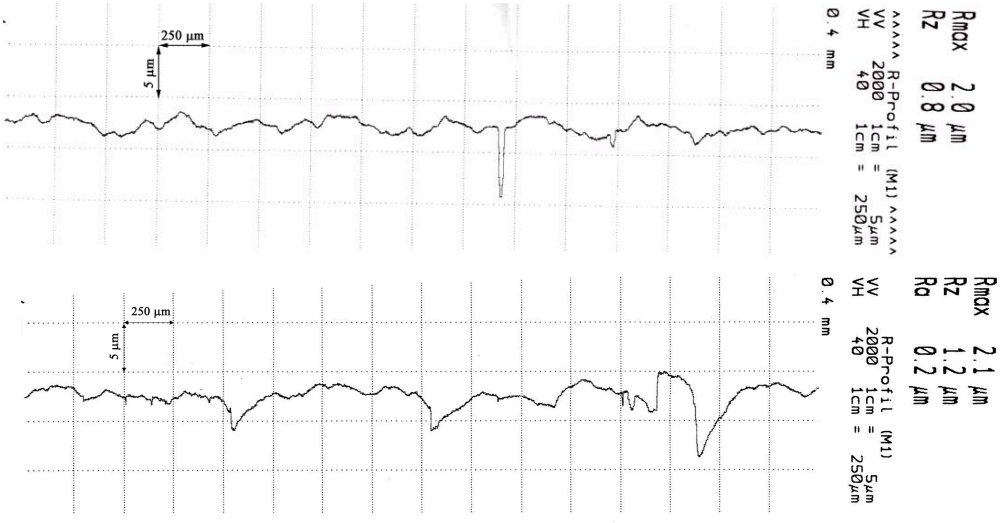

Figure 3. Surface profile development in the course of plasma exposures, Q=0.75 MJ/m^2.

Roughening of the surface caused by plasma exposures are demonstrated also by dedicated measurements with AFM (Fig.4). Specific surface morphology is developed due to the crack meshes arisen on the surface and also it is influenced by melt layer appearance and surface tension effects.

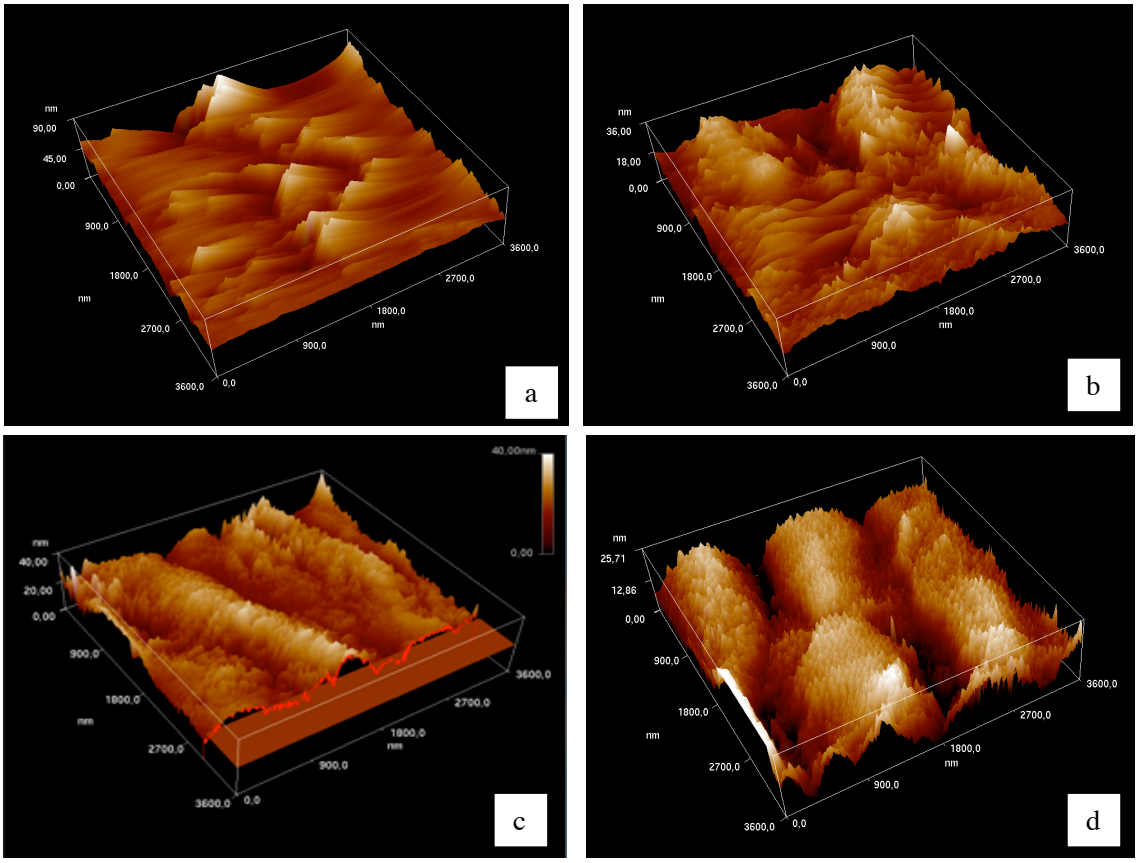

Figure 4. AFM images of single forged tungsten sample; a-initial surface, b- exposed with 10 pulses of 0.75 MJ/m^2, c,d- exposed with 20 pulses of 0.75 MJ/m^2.

Tungsten cracking leads to separation of material peaces with further ejection of erosion products from the surface. Depending of the heat load value the eroded material could be in the form of solid dust or, for exposures with melting, as splashed droplets. However, the droplets appearance is registered also in regimes of plasma exposures with the energy loads below the melting threshold. Formation of dust particles in the course of cracking and development of sharp edges of the cracks are further resulted in their melting under the plasma energy deposited because of decreased heat transfer to the bulk. Being initially solid they are subjected to melting during the later stage of plasma pulse or with next plasma impact in spite of other surface remains non melted.

Formation of dust particles in the course of surface cracking with their subsequent melting under the action of plasma pulses is shown in Fig. 5. Melting of the crack edges is also clearly observed. Performed analyses confirms that registered droplets consist of tungsten material and its appearance do not caused by other effects (e.g. from electrodes erosion, diaphragm, holder etc.).

Target preheating to 200 ºC do not resulted in suppression of tungsten cracking. Nevertheless it influences on the cracking dynamics. Cracks are starting to appear only after several pulses, they grow slower, their depth and width remain to be smaller in comparison with RT targets exposures. Some examples of surface cracks after 10 and 100 plasma pulses of 0.45 MJ/m^2 target are presented in Fig.6

for preheated to 200 °C. It is seeing that surface damage by cracking for 100 plasma pulses became more pronounced as compare to initial 10 exposures.

Detailed analysis of the crack patterns for deformed tungsten material has been performed and results of characterization of the crack meshes are summarized in Table 1. Average crack depth is grown practically twice with simultaneous increase of crack width also in 2 times. Average size of crack mesh, i.e. distance between cracks, is practically unchanged. It influenced only by some new cracks appearing on the surface and completing the crack pattern.

Element	Weight %	Atomic%
Fe K	1.12	3.56
Cu K	0.65	1.82
W M	98.22	94.62
Total	100.00	

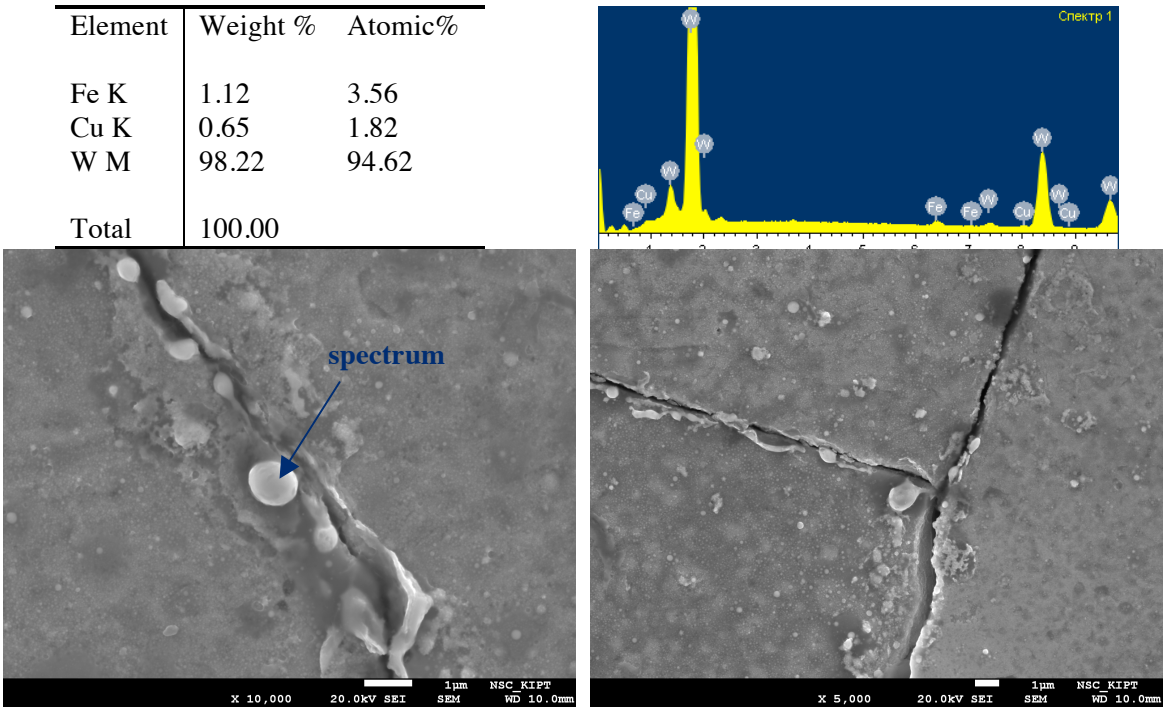

Figure 5. Formation of dust particles on DF tungsten sample in the course of surface cracking with their subsequent melting by plasma pulses. Exposition dose 400 pulses, Q=0.45 MJ/m^2.

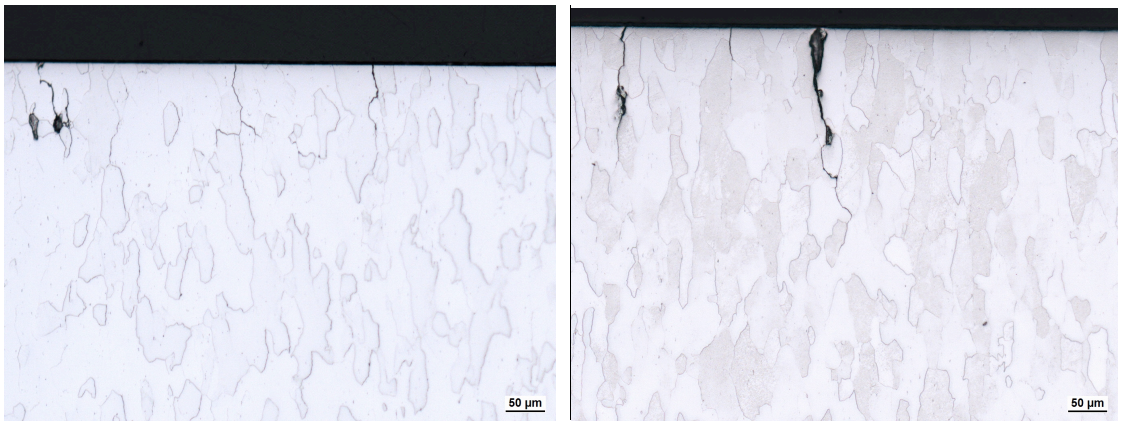

Figure 6. Comparison of surface cracks for 10 and 100 plasma pulses of 0.45 MJ/m^2. Initial temperature is 200 ^{0}C.

It should be mentioned that size of the major crack mesh is about half millimeter and it is similar for all investigated tungsten grades being characteristic of brittle destruction of W surface in the course of plasma pulses. However, major cracks that are arisen in sintered tungsten for exposed RT targets have average width of 5μm after 100 pulses and it achieved 7 microns after 300 plasma exposures.

Table 1. Characterization of crack patterns on the single forged W material exposed with 10 and 100 pulses of 0.45 MJ/m^2, T=200 ^{0}C

	Crack depth		**Crack width**		**Distance between cracks**	
	10 pulses	100 pulses	10 pulses	100 pulses	10 pulses	100 pulses
average [μm]	92.78	171.72	1.11	2.12	546.32	432.55
minimum [μm]	20.62	68.04	0.30	0.78	22.33	39.08
maximum [μm]	119.59	329.9	1.70	2.91	2171.59	1278.39
standard deviation [μm]	26.72	55.94	0.30	0.54	358.77	223.55
median [μm]	103.09	154.64	1.12	2.22	474.51	418.69

Thus, it is obtained that deformed W material is found to be more resistive against cracking and grain losses as compare to other pure W samples. No major cracks are detected after single pulse for the target preheated at 200°C. However, with further pulses, once a major crack develops for deformed W, it grows quickly and propagates transversely to the surface along the grain boundary to the depth of ≈200 μm. In result, after 100 plasma pulses of 0.45 MJ/m^2 the tungsten surface is essentially damaged by the cracks, as it is demonstrated by cross-section image in Fig.7. After 400 plasma pulses crack depth achieves ~400 μm.

Cross-section metallography shows that crack thickness can be maximal not on the surface, but in some depth below. It could be attributed to the fact, that DBTT transition under the target cooling after impacting plasma pulse occurs firstly in deeper layers, while the surface is still remained to be above DBTT. Then, cooling front achieves the surface. Therefore the crack could be originated in some depth below the surface, and the maximal width of major cracks sometimes is registered in the depth of 10-20 microns and higher, confirming this conclusion. In very deep layers the temperature changes are rather small to initiate the cracking process. Nevertheless the major crack, if arrisen, propagates to the bulk regions which were not heat affected by plasma pulses.

Figure 7. Cross-section of single forged W exposed with 100 pulses of 0.45 MJ/m^2 T=200 ^{o}C.

Cracking process is originated by the stresses which induced the plasma pulses. Residual stresses in surface layer in the course of plasma pulses were analyzed with XRD using the $\sin^2\psi$-method. Plasma irradiation results in a symmetrical tensile stress in thin subsurface layer. Maximal residual stress in the plasma affected layer is reached after first plasma pulses, and further pulses change the stress not substantially. It is observed as a rule that increase of number of exposures decreases the residual stress.

It is obtained that the residual stress does not practically depend on initial target temperature and significantly grows with increasing thermal loads up to achievement of melting threshold for exposed material. Surface melting with repetitive exposures leads to fast relaxation of stresses in the surface layer.

Results of XRD analysis of residual stresses in surface layer for DR targets exposed in different regimes are summarized in Table2. As follows from the performed measurements, the lattice parameter does not changed significantly in the course of plasma exposures. For surface heat load of 0,45 MJ/m^2 the maximum stress level in surface layer is ~400 MPa and it does not depend on the initial state (as compare DF 73 and 74). With increased number of pulses up to 100, stresses are relaxed to 270 - 284 MPa. Decreasing line width (B) as observed in result of exposures is caused by changing dislocation density in the plasma affected layer of the material. It should be mentioned that asymmetry δS (the difference between left and right side of the line profile) become negative, i.e. increasing the right-hand side is detected. This may be explained by corresponding increase in the number of interstitial complexes, which is consistent with a slight grows in the lattice parameter. For plasma exposures with Q=0,75 MJ/m^2 which are always accompanied by strong melting of the surface layer the trends are similar to those obtained for exposures with Q=0,45 MJ/m^2.

It was found that under similar loading conditions the magnitude of residual stresses for deformed tungsten material is smaller practically in 2 times in comparison with those observed for sintered samples and rolled W plates in similar conditions. The obtained result can be explained by combination of two factors: initial compressive stresses in deformed W grade and its improved structure in comparison with sintered and rolled W grades. Threshold residual stresses for cracks formation are 300-350 MPa.

Table 2. XRD analysis of stresses in surface layer for DR targets

targets	Heat load	Number of pulses	a_0, å	σ, MPa	B, degree	δS, %
DF 73	0 (initial)	0	3.1640	-33	0.56	+8
	0.45 MJ/m^2	10	3.1649	440	0.52	-3
DF 74	0 (initial)	0	3.1640	-360	0.55	+7
	0.45 MJ/m^2	10	3.1645	390	0.53	-12
DF 75	0 (initial)	0	3.1641	-380	0.56	+6
	0.45 MJ/m^2	100	3.1644	270	0.44	-7
DF 76	0 (initial)	0	3.1640	-365	0.58	+7
	0.45 MJ/m^2	100	3.1646	284	0.48	-13
DF 21	0 (initial)	0	3.1642	-47	0.5	+2
	0.75 MJ/m^2	10	3.1647	301	0.47	-1.5

Plasma exposures of WTa5 tungsten grade, that enriched be 5% of tantalum demonstrate considerably suppressed brittle destruction effects for this material with no essential influence on melting threshold energy. Repetitive plasma pulses with energy load of 0.3 MJ/m^2 do not result in

cracking development. It means that threshold load for the cracking initiation for this material is above 0.3 MJ/m^2. Due to improved ductility, no major cracks are found on the surface even for RT targets exposures with several tens pulses of 0.45 MJ/m^2 which lead to crack meshes for all other grades. For energy load of 0.45 MJ/m^2 isolated thin cracks are appeared on the surface with increasing the exposition dose up to 100 plasma pulses. Thus WTa5 shows better performance in terms of cracks due to its ductility, only single cracks which do not form the complete mesh on the surface are registered after QSPA exposures of this W grade. Fig.8 shows exposed surface after 100 plasma pulses of 0.45 MJ/m^2 with examples of droplet and arisen crack. Resulting formation of micro-sized debris separated by cracking development is also seen. Droplet is W material. However, tantalum is difficult to distinguish in the spectrum on the background of W.

Besides the erosion products in form of solid particles and droplets, the important feature of plasma-surface interaction is surface modification with formation of fine cellular structures on the surface exposed with repetitive pulses. The SEM shows that the size of cellular structure globules (up to 200 nm) is essentially less than initial size of tungsten grains. Such "foam-plastic" ordered structures of nano-size on the tungsten surface have been detected also for other W grades [18]. It is obvious, that the observed surface modification effects with formation of submicron or nano-cellular structures may play an important role in the material behaviour under the transient plasma heat loads.

Element	Weight %	Atomic%
Fe K	0.25	0.78
Cu K	2.99	8.15
W M	96.76	91.07
Total	100.00	

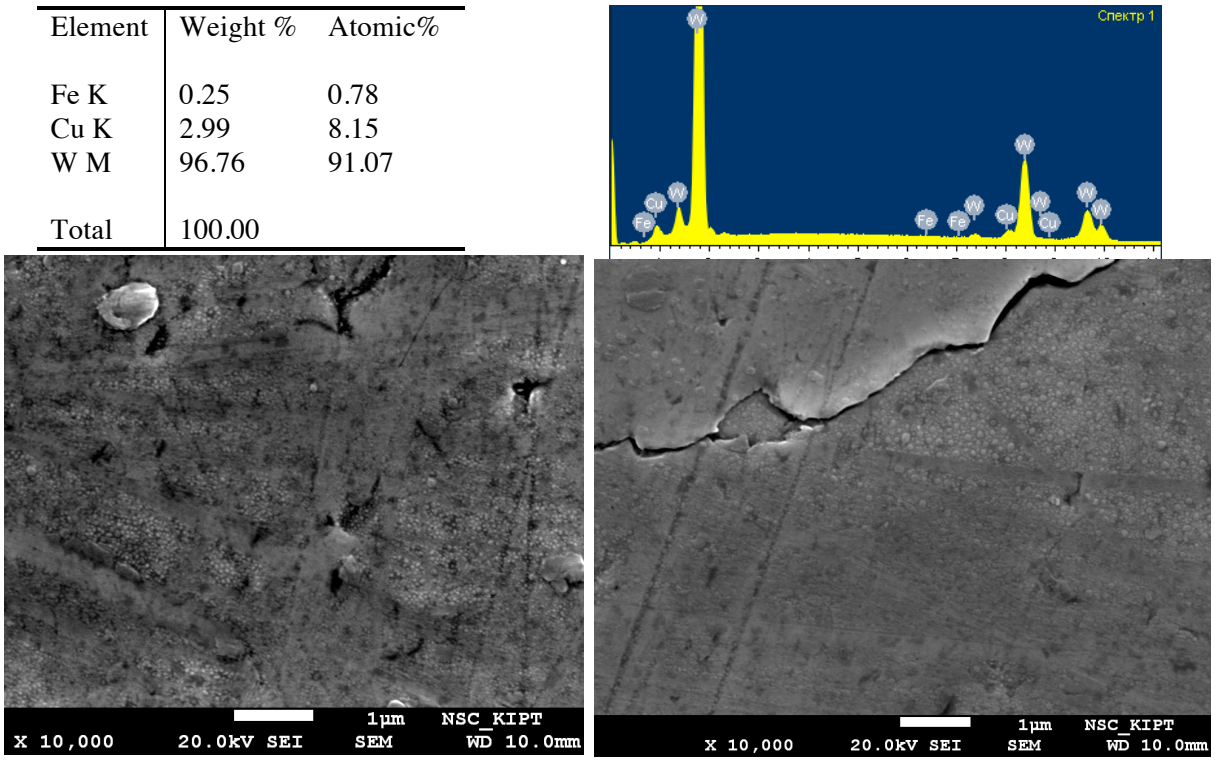

Figure 8. Surface modification of WTa5 with formation of nanosized structures and single crack, Exposition dose is 100 pulses, Q=0.45 MJ/m^2. Droplet is W material.

4. Summary

Experimental simulations of ITER-like transient events with relevant surface heat load parameters (energy density up to 1.1 MJ/m^2 and the pulse duration of 0.25 ms) as well as particle loads (varied in wide range from 10^{23} to 10^{27} ion/m^{2}s) were carried out with a quasi-stationary plasma accelerator

QSPA Kh-50. Particular attention was paid to elaboration of damage of tungsten as a main PFM for ITER divertor surfaces and also as prospective material foreseen for DEMO design.

Tungsten damage during the transient events is dominated by influence of macroscopic erosion mechanisms related with cracking development and surface melting effects.

Erosion products in the form of solid dust and splashed droplets are analyzed. Performed studies demonstrate that main sources of W dust are cracks development, resolidification process and material surface modification resulted in formation of cellular nanostructures in the course of repetitive plasma pulses.

Besides the melt motion and splashing effects for exposures with pronounced melting, the tungsten droplets appearance is registered also in regimes of plasma exposures with the energy loads below the melting threshold. It was found that main source of the droplets in this case is melting of separated material pieces and sharp crack edges. Due to decreased heat transfer to the bulk their melting occurs during later stage of plasma pulse or with next plasma impacts in spite of other surface remains solid.

For investigated pure W grades the damage threshold energy as well as the observed major cracking and roughening of the samples that exposed above these thresholds are qualitatively similar Performed experiments show just quantitative differences for the measured crack parameters. Deformed W material is found to be more resistive against cracking and grain losses as compare to other pure W samples.

The most pronounced differences of material performance are observed for W material alloyed with tantalum. Among investigated W grades WTa5 shows better performance in terms of cracks due to improved ductility. Only single isolated cracks which do not form the complete mesh on the surface are registered after QSPA exposures threshold load for the cracking initiation for this material is above 0.3-0.35 MJ/m^2 for single pulse. Threshold behaviour with multipulsed plasma exposures and possible degradation of the material properties could be a subject for further studies. It should be mentioned that even preheating up to 200 C does not result in suppressing of cracking, thus DBTT for this grade is still higher.

Within further round-robin tests, some of exposed samples could be subjected to irradiation with other involved simulators. In particular, synergetic effects would be important. Also, combination of steady state and pulsed plasma exposures is of especial interest aiming at damage character and erosion products, hydrogen retention etc. Basing on this planned activity comprehensive database on material surface characterization after exposures with different devices should be created including roughness values, crack distance, crack depth and width etc.

Acknowledgments

This work has been performed in part within IAEA CRP F1.30.13 and also partially supported by the Targeted Program of NAS of Ukraine on Plasma Physics. The authors would like to acknowledge N.V. Kulik, V.V. Staltsov, S.I. Lebedev, and P.V. Shevchuk for their assistance in the experiments.

References

[1] Philipps V 2011 *J. Nucl. Mater.* **415**, 1, Suppl 1, S2
[2] Rieth M, Armstrong D, Dafferner B, Heger S, Hoffmann A, Hoffmann M D, Jäntsch U, Kübel C, Materna-Morris E, Reiser J, Rohde M, Scherer T, Widak V and Zimmermann H 2010 *Advances in Science and Technology* **73** 11.
[3] Pintsuk G 2012 *Comprehensive Nuclear Materials* **4** 551
[4] Pitts R A, Carpentier S, Escourbiac F, Hirai T, Komarov V, Kukushkin A S, Lisgo S, Loarte A, Merola M, Mitteau R, Raffray A R, Shimada M and Stangeby P C 2011 *J. Nucl. Mater.* **415** 1, Suppl 1, S957.
[5] Landman I S, Pestchanyi S E, Safronov V M, Bazylev B N and Garkusha I E 2004 *Physica*

Scripta **T111** 206
[6] Miloshevsky G and Hassanein A 2011 *J. Nucl. Mater.* **415** 1 S74
[7] Pestchanyi S, Garkusha I and Landman I 2010 *Fusion Engineering and Design* **85** 1697
[8] Tereshin V I, Bandura A N, Bovda A M, Brown I G, Byrka O V, Chebotarev VV, Garkusha I E and Tortika A S 2002 *Review of Scientific Instruments* **73** (2) 831
[9] Loewenhoff Th, Bürger A, Linke J, Pintsuk G, Schmidt A, Singheiser L and Thomser C 2011 *Physica Scripta* **T145** 014057
[10] Skladnik-Sadowska E, Czaus K, Malinowski K, Sadowski M J, Nowakowska-Langier K, Ladygina M S and Garkusha I E 2012 *Nukleonika* **57(2)** 193
[11] Poznyak I M Arkhipov N I, Karelov S V Safronov V M and Toporkov D A 2012 *Problems of Atomic Science and Technology, Series: Plasma Physics* **6** 52
[12] Makhlaj V A, Bandura A N, Byrka O V, Garkusha I E, Chebotarev V V and Landman I S 2007 *Physica Scripta* **T128** 239
[13] De Temmerman G, Daniels J, Bystrov K, van den Berg M A and Zielinski J. 2013 *Nucl. Fusion* **53** 023008
[14] Makhlai VA, Garkusha I E , Malykhin S V, Pugachov A T, Landman I, Linke J, Pestchanyi S, Chebotarev V V and Tereshin V I 2009 *Physica Scripta* **T138** 014060
[15] Tereshin V I 1995 *Plasma Phys. Control. Fusion* **37** A177
[16] Garkusha I E, Bandura A N, Byrka O V, Chebotarev V V, Landman I, Makhlaj V A, Pestchanyi S and Tereshin V I 2009 *J.Nucl. Mater.* **386-388** 127
[17] Wirtz M, Linke J, Pintsuk G, Singheiser L and Uytdenhouwen I. 2011 Comparison of the thermal shock performance of different tungsten grades and the influence of microstructure on the damage behaviour *Physica Scripta T145* 014058
[18] Makhlaj V A, Garkusha I E, Aksenov N N, Chuvilo A A, Chebotarev V V, Landman I. Malykhin S.V. Pestchanyi S and Pugachov A T 2013 *J. Nucl. Mater.* **438** S233